coatings

Communication

Characterizing the Thermally Grown Oxide in Thermal Barrier Coating by Terahertz Time Domain Spectroscopy

Wenhan Zhao [1], Shibin Wang [2], Lin'an Li [2], Delin Liu [2], Chuanwei Li [2,*] and Zhiyong Wang [2,*]

[1] Department of Mechanics, Tianjin University, Tianjin 300072, China
[2] Aviation Key Laboratory of Science and Technology on Advanced Corrosion and Protection for Aviation Material, Beijing Institute of Aeronautical Materials, Beijing 100094, China
* Correspondence: licw16@tju.edu.cn (C.L.); zywang@tju.edu.cn (Z.W.)

Abstract: This paper presents a method to simultaneously measure the thickness and refractive index of the thermally grown oxide (TGO) in thermal barrier coating (TBC) by using a reflective terahertz time-domain spectroscopy (THz-TDS) system. First, an optical transmission model of THz radiation in the multilayer structure of TBC is established. Owing to the different structures of TBC before and after forming the TGO layer, two different transmission models are established, respectively. Then, the experimental signals from the samples after different thermal cycles are obtained by the THz-TDS system. By fitting the experimentally measured reflected THz signals from the TBC samples to the proposed optical model using an optimization algorithm, the thickness and refractive index of the TGO are determined. In this work, four samples with different thicknesses of TGO layers are analyzed. The results of thickness of TGO layer are verified by SEM observation, and a reasonable agreement is obtained.

Keywords: non-destructive; thermal barrier coatings; terahertz time-domain spectroscopy; thermally grown oxide; optimization algorithm; SEM observation

check for updates

Citation: Zhao, W.; Wang, S.; Li, L.; Liu, D.; Li, C.; Wang, Z. Characterizing the Thermally Grown Oxide in Thermal Barrier Coating by Terahertz Time Domain Spectroscopy. *Coatings* **2023**, *13*, 376. https://doi.org/10.3390/coatings13020376

Academic Editor: Narottam P. Bansal

Received: 9 January 2023
Revised: 30 January 2023
Accepted: 2 February 2023
Published: 7 February 2023

1. Introduction

Due to the merits of ceramic oxides, such as high thermal, wear and electrical resistances, thermal barrier coating (TBC) composed of ceramic oxides is a common technique to keep the substrate from mechanical wear and thermal shock [1–3]. TBC is a multi-layer composite material including topcoat (TC), bond coat (BC), and substrate. For TBC working on cycling thermal shock, it is almost unavoidable to generate thermally grown oxide (TGO) between TC layer and BC layer due to the oxidation of the metallic element in the BC layer [4,5]. Furthermore, the thickness of TGO will increase with its working time. The generated TGO will introduce extra stress into TBC. It has been proven that the stress induced by TGO is an important factor of TBC failure. In order to predict the service life of TBC without destroying its structure, scholars use various techniques to research TBC and TGO.

In 2004, Sugasawa et al. established a model to analyze the behavior of bulk ultrasonic waves in sprayed coating layers. Using this model, the sound speed can be determined if the coating thickness is known, and vice versa. According to their reports, the spatial resolution of this method is about tens of micros. Thus, this method should be applicable to measure the thickness of TBC, but not TGO. This is because the typical thickness of TGO is about several micros [6]. In 2017, Shrestha et al. used thermal wave imaging to evaluate non-uniform coating thickness, with a measurement accuracy of about several microns [7,8]. However, they did not demonstrate the ability of this method on the thickness measurement of TGO. In 2019, Wang et al. developed a method to non-destructively evaluate the thickness of TGO by using impedance spectroscopy [9].

Terahertz time-domain spectroscopy (THz-TDS) has recently emerged as a new non-destructive testing method. Due to excellent penetrability of terahertz (THz) radiation for ceramics, it is a powerful tool for non-destructive analysis of the coatings in TBC [10,11]. In 2009, White et al. adopted THz-TDS imaging to map the thickness of yttria stabilized zirconia (YSZ) in TBC, and thermal degradation was observed [12]. In 2010, Chen et al. observed the relevance between the phase delay of THz pulse and the SEM-determined TGO thickness [13]. In 2014, Fukuchi et al. measured the refractive index and thickness of the TC layer in TBC using reflective THz radiation [14].

Although this excellent work has demonstrated the measurement capability of THz radiation on the structure of TBC, the accurate thickness of the TGO layer has not been steadily measured by the THz method until now. Based on the previous work, to obtain more accurate information regarding the TGO layer, this paper analyses the experimental signal and the simulated signal, combines with SEM results, and speculates on the thickness and refractive index of the TGO layer. The rest of this paper is organized as follows. Section 2 introduces the measurement principle and experimental process. The experimental results and simulated results are provided in Section 3. Section 4 presents the conclusions.

2. Methods

In this work, a typical all-fiber reflective THz-TDS system was used. The working parameters ((Menlo Systems, Munich, Germany)manufacturer, city, state (only for USA and Canada), country) of the femtosecond laser adopted in the THz-TDS system were as follows: repetition rate 100 MHz (±1 MHz), wavelength 780 nm (±30 nm), power more than 330 mw, pulse width less than 100 fs. Two photoconductive antennas were used to emit and receive THz radiation. The spot diameter of the THz radiation was about 5 mm, and its reliable frequency was in the range 0.3 THz~1.5 THz. The experimental temperature was controlled at 20 °C. A double-sided polished high resistance silicon was used as a beam splitter. Figure 1 shows the schematic diagram of the experimental setup.

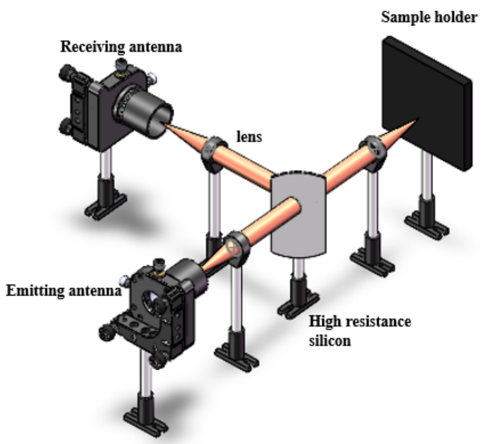

Figure 1. Schematic diagram of the experimental setup.

Electron Beam Physical Vapor Deposition (EBPVD) technology was used to prepare the TBC samples. The material of the TC layer in this work was 8YSZ (ZrO_2-8 wt.%Y_2O_3), and nickel-based alloy which contains nickel, chromium, aluminum, yttrium, and hafnium composed the BC layer. To prepare the samples containing TGO layer, the initial TBC samples were subjected to 500, 1000, 2000, 5000 thermal cycles. As the time of thermal cycle increases, the TGO layer continues growing. This newly generated TGO layer changes TBC from the initial three-layer structure to a four-layer structure.

The schematic diagram of the THz propagation path in a sample is shown in Figure 2 [15]. Both of the distances between R_0 and R_1, R_1 and R_2 mean the transmission process of THz radiation in TC layer, so that the Δt between them are equivalent. The formula between thickness and the refractive index of TC layer can be expressed as

$$d = \frac{c\Delta t}{2n} \quad (1)$$

where n represents the refractive index, d denotes the thickness, c denotes the speed of the light in vacuum and Δt denotes the time delay of THz radiation in the TC layer.

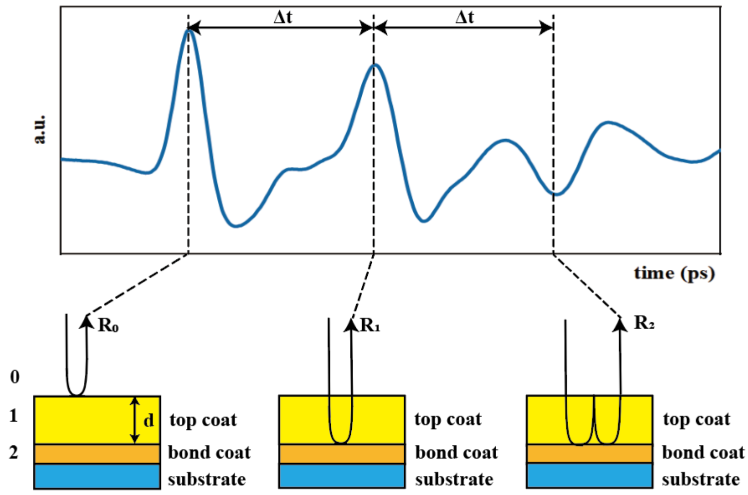

Figure 2. Schematic diagram of the THz propagation path in a sample.

Figure 3 shows the initial and after thermal cycling multi-layer structures of the TBC samples, and the different propagation path of THz radiation in the samples. The samples used in this paper are prepared in the same batch. TC layers are considered to have the same thickness. Therefore, to get the information regarding the TGO layer with high reliability, the thickness of the TC layer is firstly determined in advance using the as-prepared samples.

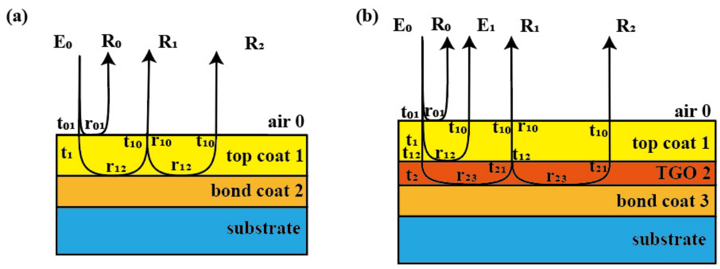

Figure 3. (**a**) Structure of the TBC before thermal cycle; (**b**) Structure of the TBC after thermal cycle.

As shown in Figure 3a, in the initial TBC, the THz radiation emitted from the emitting antenna is represented as E_0. The signal obtained after reflection on the surface of the TBC is represented as R_0. R_1 and R_2 are the first and second reflected signals from the interface between TC layer and BC layer, respectively.

Similarly, in Figure 3b, R_0 represents the surface reflection of TBC after thermal cycle. E_1 is the reflected signal from the interface between TC and TGO layer. R_1 represents the interface reflection of TGO and BC layer, and R_2 represents the second reflection which travels through the ceramic layers twice.

According to Fresnel formula, we have

$$t_{ij} = \frac{2n_i}{n_i + n_j} \quad (2)$$

and

$$r_{ij} = \frac{n_i - n_j}{n_i + n_j} \quad (3)$$

where t_{ij} and r_{ij} (i, j = 0, 1, 2, 3) are the Fresnel transmissive and reflective coefficients, respectively, of each interface and 0 represents air, 1 the TC layer, 2 the BC layer (in Figure 3a) and the TGO layer (in Figure 3b), 3 the BC layer (in Figure 3b). Let t_i (i = 1, 2) represent the transmission coefficient of each layer, where 1 represents the TC layer, and 2 the TGO layer (in Figure 3b). Further, $t_i = \varepsilon_i d_i$, where ε_i denotes the absorption coefficient per unit length in the sample, d_i denotes the thickness.

Using the transmissive and reflective coefficients, the signal from the as-prepared sample can be expressed as follows

$$S_{initial} \approx R_0 + R_1 + R_2 = E_0\left(r_{01} + t_{01}t_{10}r_{12}t_1^2 + t_{01}t_{10}r_{12}^2 r_{10}t_1^4\right) \quad (4)$$

The signals such as the signal reflected from the interface between TC and TGO is too small, so that it is difficult to distinguish the interface signal of TGO/BC from the noise (a conclusion derived from experimental results). Meanwhile, because of the relatively thin thickness of TGO layer, the time delay between E_1 and R_1 is too close. Therefore, the primary and secondary reflection of the interface are mainly studied in this paper. The expressions of the subsequent signals are omitted. Finally, the expressions of the samples after the thermal cycles are as follows

$$S_{tgo} \approx R_0 + E_1 + R_1 + R_2 = E_0\left(r_{01} + t_{01}t_{10}r_{12}t_1^2 + t_{01}t_{12}r_{23}t_{21}t_{10}t_1^2 t_2^2 + t_{01}r_{10}t_{10}t_{12}^2 r_{23}^2 t_{21}^2 t_1^4 t_2^4\right). \quad (5)$$

The optimization algorithm adopted in this paper to obtain the minimum error between the experimental signal and the simulation signal is defined as follows

$$\delta = \Sigma(m_e - m_s)^2, \quad (6)$$

where δ represents the sum of the squares of the difference between experimental results and simulation results, m_e represents the experimental results, and m_s represents the simulation results. By the optimization search on the error function, the thickness and refractive indexes of TC and TGO can be determined. Here, we have obtained the simulated signals of the as-prepared sample and the sample after thermal cycle, respectively, and then collected the corresponding experimental signals.

By selecting the suitable range of refractive index and thickness, the δ mentioned previously can be calculated by the algorithm. After comparing the different δ, the minimum can be obtained and the corresponding indexes are considered to be the final result.

3. Results and Discussion

In this work, to determine the thickness and refractive index of the TC and TGO layers, the experimental measurement is carried out in two steps. The as-prepared sample is measured at first to obtain the thickness and refractive index of the TC layer. Then, indexes obtained by last step are used as the known quantities for the samples after thermal cycle. Repeating the calculating process in samples after thermal cycle, the relevant indexes of TGO layer can be finally acquired.

In order to simulate the reflective signals from the samples, an air signal of the THz-TDS system is needed as the reference signal, as shown in Figure 4a. Then, the samples are fixed on the sample holder. By adjusting the position of holder, the focus of the THz radiation is just on the surface of the sample. A captured THz signal of the as-prepared sample and the simulated result are shown in the Figure 4e. Figure 4f shows the difference between simulation and measurement.

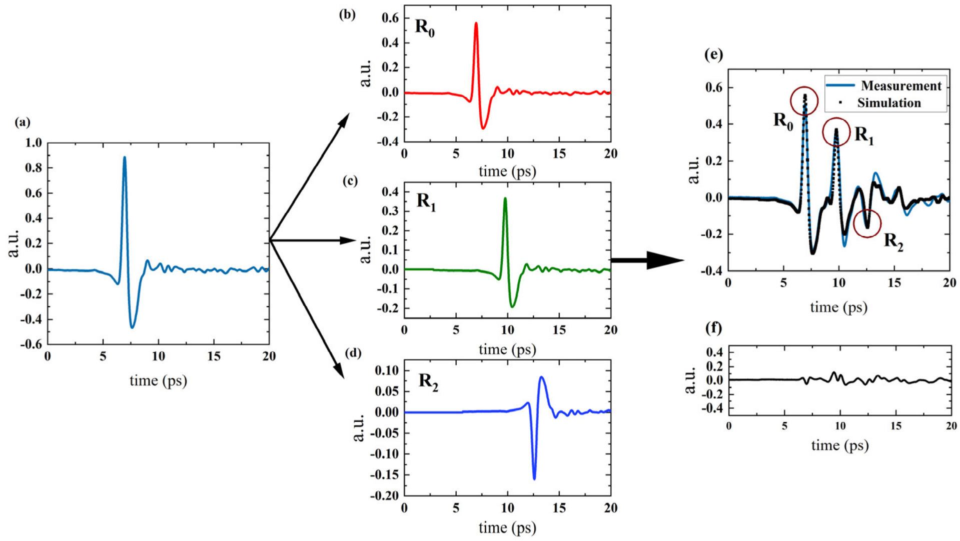

Figure 4. (**a**) The used reference signal obtained by reflective THz experimental platform; (**b**) Simulated signal of R_0 (the surface reflection); (**c**) Simulated signal of R_1 (the first interface reflection); (**d**) Simulated signal of R_2 (the second interface reflection); (**e**) Comparison between the simulated result and the experimental result; (**f**). The difference between the two signals.

Figure 4b–d shows the simulated signals R_0, R_1 and R_2, whose combination obtains the closest fitting to the experimentally captured reflected signal from the as-prepared sample. The closest fitting is obtained when the refractive index takes 4.45, and the thickness of the TC layer takes 95 µm [15]. As indicated in Figure 4e,f, the simulated signal is well fitted with the experimental signal. In addition, from Figure 4e, we know that TC layer is thick enough so that the peaks from the different reflected signals are distinguishable.

To ensure the accuracy of the thickness acquired by the algorithm, all the samples used in this paper are cut for the SEM observation. HITACHI S-4800 Field Emission Scanning Electron Microscope (Hitachi Limited, Tokyo, Japan) is used for microscopic observation. The microscope image of the as-prepared sample is shown in Figure 5 that shows the thickness of the TC layer is about 94.1 µm. The SEM result matches the results obtained by the proposed THz method well. Each sample was tested five times, and the obtained results were analyzed with the SEM measurement results. Meanwhile, to minimize the error, the experimental signals are averaged after 100 scans. Finally, the measurement standard deviation of the as-prepared sample is 0.6893.

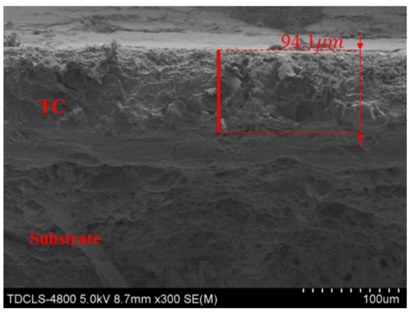

Figure 5. The TBC result of the SEM.

Figure 6 shows the experimental and simulated signals from the TBC samples after 1000 thermal cycles. As shown in Figure 6c, the signal of E_1 represents the reflection from the TC/TGO interface. Because the refractive indices of the TC and TGO layers are relatively close to each other, the Fresnel reflective coefficient between them is low. This is the reason why the amplitude of E_1 is small. Therefore, the second reflected signal from the TC/TGO interface is not taken in account in the theoretical model of this work. The closest model fitting result is obtained when the refractive index and the thickness of TGO layers takes 4.54 and 4.71 μm, respectively.

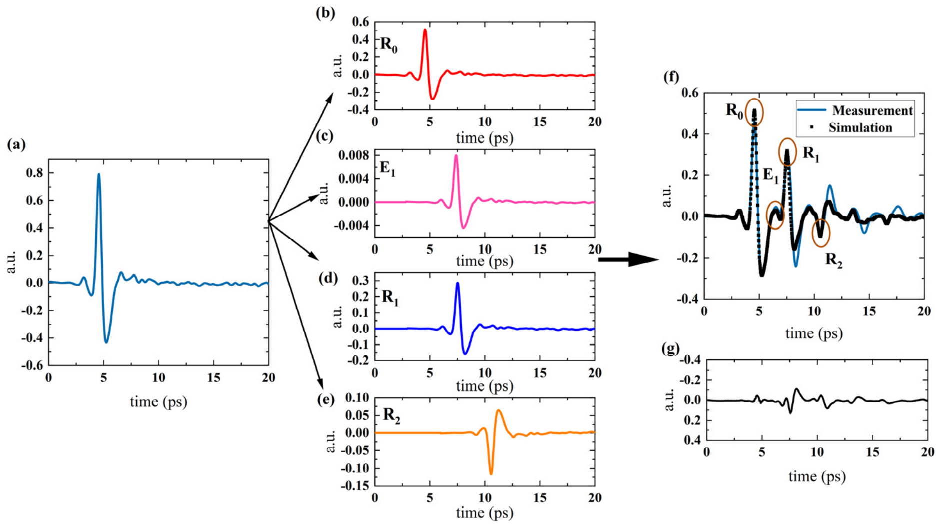

Figure 6. (**a**) The used reference signal obtained by reflective THz experimental platform; (**b**) Simulated signal of R_0 (the surface reflection); (**c**) Simulated signal of E_1 (the TC/TGO interface reflection); (**d**) Simulated signal of R_1 (the first TGO/BC interface reflection); (**e**) Simulated signal of R_2 (the second TGO/BC interface reflection); (**f**) Comparison between the simulated result and the experimental result; (**g**) The difference between the two signals.

Other thermal cycling samples are also analyzed using the above experimental process, and the optimization algorithm is also used in the samples to obtain the refractive index and thickness. Meanwhile, to verify the refractive index, the SEM results are put into the optimization algorithm. The results are listed in Table 1. As shown in Table 1, the maximum relative error of the refractive index is not more than 5%, which shows a good consistency. The error may be caused by the experimental environment, the experimental process and the algorithm itself. THz radiation is easily affected by the water vapor in the air which may lead to the occurrence of scattering. A slight shift in the position of the experimental platform during sample replacement will also bring in some measurement errors.

Table 1. The results of the measurement and SEM observation about TGO.

	Thermal Cycles	**500**	**1000**	**2000**	**5000**
THz-TDS	Refractive Index	4.57	4.54	4.51	4.55
Measurement	Thickness (μm)	4.11	4.71	5.58	6.34
SEM Observation	Thickness (μm)	4.22	4.72	5.82	6.41
	Standard Deviation	0.8650	0.8423	0.8921	0.8842
	Refractive Index (Verification)	4.45	4.53	4.32	4.51
	Relative Error (of Refractive Index)	2.6%	0.2%	4.3%	0.8%

Meanwhile, the comparison between THz measurement and SEM observation regarding the thickness of the TGO layer is shown in Figure 7. Both results indicate that the increasing rate of the TGO thickness decreases gradually with the increase of the thermal cycling times. The reason is that in the initial stage of the thermal cycle, the contact area between BC layer and external environment is still relatively large. When the alumina grows to a certain extent, the contact area between the BC layer and air shrinks which causes the reaction speed to slow down [16]. The refractive indices of the generated TGO layer are almost constant, as shown in Table 1. Figure 8 presents the SEM images of those samples.

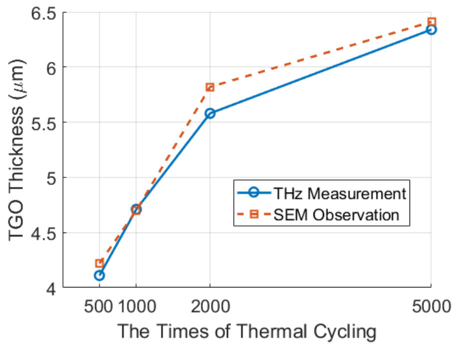

Figure 7. The thickness of the TGO layers after different thermal cycles.

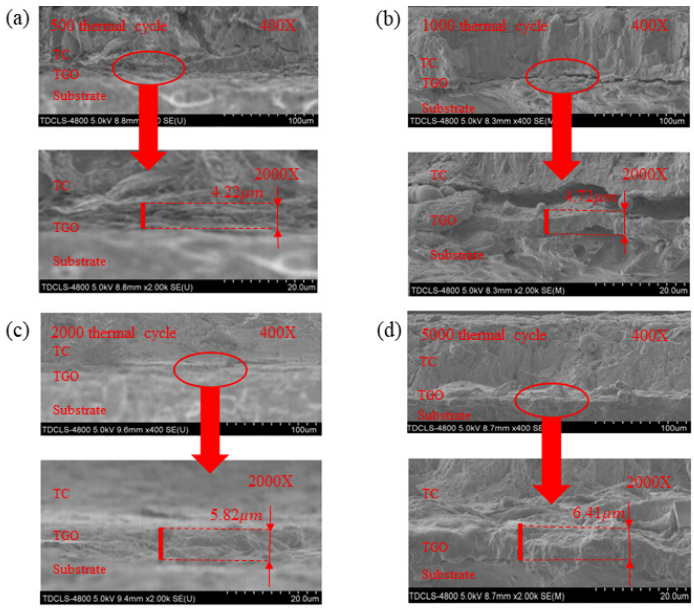

Figure 8. (**a**) The SEM results of the sample after 500 thermal cycles; (**b**) after 1000 thermal cycles; (**c**) after 2000 thermal cycles; (**d**) after 5000 thermal cycles.

Figure 9 shows the distribution of the δ in Equation (6). As shown in Figure 9, it can be seen that the distribution is continuous, smooth, and has only one local minimum. It is proved that the δ has a unique convergence value. Therefore, the global minimum of the δ which represents the best fitting result can be found. The proposed algorithm to determine the thickness and the refractive index should be robust.

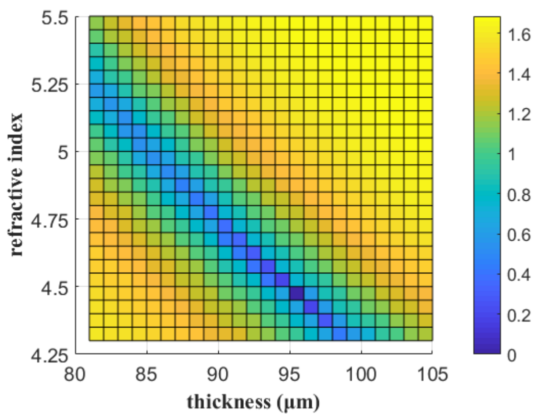

Figure 9. The distribution of the δ in Equation (6).

4. Conclusions

In this work, a reflective THz-TDS system is used to obtain the reference signal and experimental signal by measuring air and the TBC samples with different times of thermal cycle, respectively. Then, a model which shows the transmission of THz radiation in the TBCs is established. After simulating the transmission, the simulation signals of the samples before and after thermal cycle have been obtained. By comparing the simulated signals and experimental signals, an optimization algorithm which can get two kinds of signal interpolation squares is developed to evaluate the quality of the simulated signal. The minimum of the optimization algorithm means the simulation results attain the best effect. At this time, the refractive index and thickness in the simulation results are considered to be the real refractive index and thickness of TGO. To verify the validity of the algorithm, all samples are detected by the SEM. Before the SEM experiment, to get a better revivification of the working environment of the TBC, a wire-electrode cutting is used to cut the samples to expose the internal structure. By comparing the SEM results and experimental results, the accuracy of the algorithm is confirmed. Finally, the thickness of the TGO layer can be obtained by the optimization algorithm. Because of its nondestructive and nonionizing features, THz radiation is expected to be used in further research regarding TBC, such as predicting the service life and evaluating failure.

Author Contributions: Conceptualization, W.Z.; Methodology, W.Z.; Supervision, Z.W.; Writing—Original Draft Preparation, Z.W.; Writing—Review & Editing, Z.W.; Funding Acquisition, S.W.; Data Curation, L.L.; Validation, C.L.; Investigation, D.L. All authors have read and agreed to the published version of the manuscript.

Funding: The authors are grateful for the financial support from the National Natural Science Foundation of China (Grant Nos. 12041201, 12172251, and 12021002).

Institutional Review Board Statement: Not applicable.

Informed Consent Statement: Not applicable.

Data Availability Statement: All data that support the findings of this study are included within the article.

Acknowledgments: The authors are grateful to Department of Materials, Tianjin University.

Conflicts of Interest: The authors declare no conflict of interest.

References

1. Godiganur, V.S.; Nayaka, S.; Kumar, G.N. Thermal barrier coating for diesel engine application—A review. In Proceedings of the 4th International Conference on Advanced Research in Mechanical, Materials and Manufacturing Engineering (ICAMMME), Bengaluru, India, 10–11 July 2020.
2. Schulz, U.; Leyens, C.; Fritscher, K.; Peters, M.; Saruhan-Brings, B.; Lavigne, O.; Dorvaux, J.-M.; Poulain, M.; Mévrel, R.; Caliez, M. Some recent trends in research and technology of advanced thermal barrier coatings. *Aerosp. Sci. Technol.* **2003**, *7*, 73–80. [CrossRef]
3. Padture, N.P. Advanced structural ceramics in aerospace propulsion. *Nat. Mater.* **2016**, *15*, 804–809. [CrossRef] [PubMed]
4. Padture, N.P.; Gell, M.; Jordan, E.H. Thermal Barrier Coatings for Gas-Turbine Engine Applications. *Science* **2002**, *296*, 280–284. [CrossRef] [PubMed]
5. Clarke, D.R.; Levi, C.G. Materials design for the next generation thermal barrier coatings. *Annu. Rev. Mater. Res.* **2003**, *33*, 383–417. [CrossRef]
6. Sugasawa, S. Measurements of elastic properties of plasma-sprayed coatings using bulk ultrasonic pulses. *Jpn. J. Appl. Phys.* **2004**, *43*, 3109–3114. [CrossRef]
7. Shrestha, R.; Kim, W. Evaluation of coating thickness by thermal wave imaging: A comparative study of pulsed and lock-in infrared thermography—Part I: Simulation. *Infrared Phys. Technol.* **2017**, *83*, 124–131. [CrossRef]
8. Shrestha, R.; Kim, W. Evaluation of coating thickness by thermal wave imaging: A comparative study of pulsed and lock-in infrared thermography—Part II: Experimental investigation. *Infrared Phys. Technol.* **2018**, *92*, 24–29. [CrossRef]
9. Wang, Z.; Zhao, M.; Wu, R.; Xing, Y.; Yang, J.; Wang, M.; Li, Z.; Song, N.; Wan, C.; Pan, W. Non-destructive evaluation of thermally grown oxides in thermal barrier coatings using impedance spectroscopy. *J. Eur. Ceram. Soc.* **2019**, *39*, 5048–5058. [CrossRef]

10. Fan, W.H.; Burnett, A.; Upadhya, P.C.; Cunningham, J.; Linfield, E.H.; Davies, A.G. Far-infrared spectroscopic characterization of explosives for security applications using broadband terahertz time-domain spectroscopy. *Appl. Spectrosc.* **2007**, *61*, 638–643. [CrossRef] [PubMed]
11. Kojima, S.; Tsumura, N.; Kitahara, H.; Takeda, M.W.; Nishizawa, S. Terahertz time domain spectroscopy of phonon-polaritons in ferroelectric lithium niobate crystals. *Jpn. J. Appl. Phys.* **2002**, *41*, 7033–7037. [CrossRef]
12. White, J.; Fichter, G.; Chernovsky, A.; Whitaker, J.F.; Das, D.; Pollock, T.M.; Zimdars, D.; Thompson, D.O.; Chimenti, D.E. Time Domain Terahertz Non-Destructive Evaluation of Aeroturbine Blade Thermal Barrier Coatings. In Proceedings of the 35th Annual Review of Progress in Quantitative Nondestructive Evaluation, Chicago, IL, USA, 20–25 July 2008.
13. Chen, C.-C.; Lee, D.-J.; Pollock, T.; Whitaker, J.F. Pulsed-terahertz reflectometry for health monitoring of ceramic thermal barrier coatings. *Opt. Express* **2010**, *18*, 3477–3486. [CrossRef] [PubMed]
14. Fukuchi, T.; Fuse, N.; Okada, M.; Ozeki, T.; Fujii, T.; Mizuno, M.; Fukunaga, K. Topcoat Thickness Measurement of Thermal Barrier Coating of Gas Turbine Blade Using Terahertz Wave. *Electr. Eng. Jpn.* **2014**, *189*, 1–8. [CrossRef]
15. Fukuchi, T.; Fuse, N.; Okada, M.; Fujii, T.; Mizuno, M.; Fukunaga, K. Measurement of Refractive Index and Thickness of Topcoat of Thermal Barrier Coating by Reflection Measurement of Terahertz Waves. *Electron. Commun. Jpn.* **2013**, *96*, 37–45. [CrossRef]
16. Chen, W.R.; Archer, R.; Huang, X.; Marple, B.R. TGO Growth and Crack Propagation in a Thermal Barrier Coating. *J. Therm. Spray Technol.* **2008**, *17*, 858. [CrossRef]